Nanoparticles as Drug Delivery System against Tuberculosis in Zebrafish Embryos: Direct Visualization and Treatment

Federico Fenaroli,[†,⊥] David Westmoreland,[†,⊥] Jørgen Benjaminsen,[†] Terje Kolstad,[†] Frode Miltzow Skjeldal,[†] Annemarie H. Meijer,[‡] Michiel van der Vaart,[‡] Lilia Ulanova,[†] Norbert Roos,[†] Bo Nyström,[§] Jon Hildahl,[†] and Gareth Griffiths[†,*]

[†]Department of Biosciences, University of Oslo, Blindernveien 31, 0371 Oslo, Norway, [‡]Institute of Biology, Leiden University, Einsteinweg 55,2333 CC Leiden, The Netherlands, and [§]Department of Chemistry, University of Oslo, Sem Sælands vei 26, 0371 Oslo, Norway. [⊥]These authors contributed equally.

ABSTRACT Nanoparticles (NPs) enclosing antibiotics have provided promising therapy against *Mycobacterium tuberculosis* (Mtb) in different mammalian models. However, the NPs were not visualized in any of these animal studies. Here, we introduce the transparent zebrafish embryo as a system for noninvasive, simultaneous imaging of fluorescent NPs and the fish tuberculosis (TB) agent *Mycobacterium marinum* (Mm). The study was facilitated by the use of transgenic lines of macrophages, neutrophils, and endothelial cells expressing fluorescent markers readily visible in the live vertebrate. Intravenous injection of Mm led to phagocytosis by blood macrophages. These remained within the vasculature until 3 days postinfection where they started to extravasate and form aggregates of infected cells. Correlative light/electron microscopy revealed that these granuloma-like structures had significant access to the vasculature. Injection of NPs induced rapid uptake by both infected and uninfected macrophages, the latter being actively recruited to the site of infection, thereby providing an efficient targeting into granulomas. Rifampicin-loaded NPs significantly improved embryo survival and lowered bacterial load, as shown by quantitative fluorescence analysis. Our results argue that zebrafish embryos offer a powerful system for monitoring NPs *in vivo* and rationalize why NP therapy was so effective against Mtb in earlier studies; bacteria and NPs share the same cellular niche.

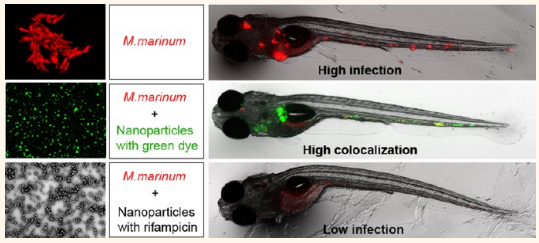

KEYWORDS: PLGA nanoparticles · drug delivery · zebrafish · fish tuberculosis · fluorescent imaging

The global burden of tuberculosis (TB) caused by *Mycobacterium tuberculosis* (Mtb) infection is alarmingly high, with 8.6 million new cases and 1.3 million deaths in 2012 (WHO report, 2013: http://www.who.int/tb/publications/global_report/en/). Infection starts in the lungs where Mtb first infects resident alveolar macrophages and subsequently newly recruited macrophages, coming from the blood, reach the site of infection. Bacterial growth slows with the onset of adaptive immunity. This process leads to the formation of an organized structure, the granuloma, considered the hallmark of tuberculosis, which consists of aggregated macrophages in different stages of infection surrounded by cells of the adaptive immune system.[1,2] This structure can remain "silent" throughout the whole life of an individual but can be reactivated by various conditions to stimulate new bacterial growth and infect new patients, even after decades.[3] The only effective treatment involves the oral administration over a total of 6−8 months of four drugs: rifampicin, isoniazid, ethambutol, and pyrazinamide. This treatment is often accompanied by side effects, such as liver toxicity, leading to patient noncompliance. This, in turn, facilitates the selection of multi-drug-resistant (MDR) strains of Mtb and more seriously extensively drug-resistant Mtb (XDR) that are resistant to additional second line antibiotics (WHO report, 2013).

There is an urgent need for new strategies to combat the disease. Multiple new drugs are in the pipeline, and many groups are trying to develop better vaccines, but

* Address correspondence to g.w.griffiths@ibv.uio.no.

Received for review April 7, 2014 and accepted June 19, 2014.

Published online June 19, 2014
10.1021/nn5019126

neither route is guaranteed success.[4] The current approaches for administering antibiotics, and indeed almost all medicinal drugs, result in a systemic delivery of the drugs throughout the body; the drugs are rapidly detoxified and/or excreted, making it necessary for daily administration. An alternative, more attractive strategy, is to encapsulate the drug inside biodegradable polymeric or lipid nanoparticles (NPs) that are selectively targeted to the cells of interest, where they can then release the drug in a sustained fashion over relatively long periods. Extensive studies with model particles such as latex beads have shown that macrophages are very efficient at phagocytosing any particle between approximately 0.2 and 6 μm that is positively or negatively charged or hydrophobic.[5,6] An obvious advantage in developing NP therapy against Mtb is that the macrophages are precisely the cells where the bacteria reside.[7] Thus, even without any specific targeting information, one would expect that, if present in the circulatory system, NPs should be efficiently targeted to macrophages of an Mtb-infected animal. This is the most likely explanation for the impressive therapeutic results that have been demonstrated using NPs, as well as larger microparticles, enclosing antibiotics against TB in animal models by different groups, most prominently that of Khuller.[8−10] Most of these studies used NPs prepared with the biodegradable polymer poly(D,L-lactic acid-*co*-glycolic acid) (PLGA). Different antibiotics have been used successfully in these studies, but the most widely used one has been rifampicin in both cultured macrophages[8] and animal models, especially mice and guinea pigs.[11] Despite these impressive results, no attempts were made to follow the fate of NPs in any TB study until now.

We recently made a detailed analysis of the encapsulation of the green dye, coumarin 6 (for localization), or rifampicin (for therapy) in PLGA NPs that were tested in cultured mouse primary macrophages infected with *M. bovis* bacillus Calmette-Guerin (BCG). These studies showed that the green NPs localized within the cells that were infected with red BCG; however, whereas the BCG resided in an arrested early phagosome, the green NPs were localized to a phago-lysosome compartment. Nevertheless, provided that sufficient rifampicin could be loaded into the PLGA NPs, the antibiotic was slowly released from the NPs and was able to completely clear the BCG infection within 9−12 days.[12]

Here, we used coumarin 6 (green fluorescent dye), rhodamine 800 (far-red fluorescent dye), or the rifampicin-loaded PLGA NPs, in conjunction with the zebrafish model of TB pioneered by the Ramakrishnan group.[13,14] This system uses the close relative to Mtb, *M. marinum* (Mm), which express red or green fluorescent proteins. In the larval stage, zebrafish embryos have an innate immune system similar to mammals but acquire an adaptive immune system only after 4−6 weeks of development.[15] When bacteria are injected into the early zebrafish embryo, which is optically transparent, they are taken up rapidly by macrophages, which are functionally active within 24 h after embryo fertilization.[15] These cells are described to carry the bacteria deep into the tissues, where they assemble into clearly visible, granuloma-like structures that resemble the granulomas seen in lungs of human TB patients.[16] By combining fluorescent Mm and NPs, we were also able to visualize fluorescent phagocytes simultaneously and noninvasively in real time by fluorescence microscopy. Our analysis was further facilitated by the availability of transgenic zebrafish having fluorescently labeled macrophages, endothelial cells, and neutrophils. Our results provide a simple rationale for why earlier efforts at NP−antibiotic therapy against Mtb were so promising in different mammalian systems; both mycobacteria and NPs reside in macrophages.

RESULTS

M. marinum Infection and Localization of Nanoparticles. We first established Mm infection of zebrafish embryos by injecting DsRed-expressing fluorescent bacilli into the posterior (caudal) cardinal vein at 48−52 h postfertilization. The outcome of the infection was similar to the results obtained by Davis *et al.*,[13] with an acute infection that is able to kill the fish within 2 weeks, depending on the number of bacteria injected. Figure 1A shows a fish that at 5 days postfertilization (dpf) has been infected with ≈150 Mm for 3 days. Already at this stage it is possible to observe the presence of cell aggregates forming an early granuloma (Figure 1B,C) and scattered infected cells (Figure 1D).

We next investigated the fate of PLGA NPs (mean diameter 316 nm), which were rendered green fluorescent using the encapsulated dye coumarin 6[12] by injection into the caudal vein 3 days after infection. The images taken at 4 days postinfection (dpi) show that green NPs efficiently localized in the vicinity with the red Mm (Figure 1E). When the embryos were monitored at higher magnification, it was evident that the NPs appeared to be in the same granuloma, likely in the same cells as the bacteria (Figure 1F−H).

M. marinum and Nanoparticles Colocalize in Macrophages. Clay *et al.*[17] identified the cells that phagocytosed intravenously injected Mm in zebrafish as macrophages by immunolabeling the cells with L-plastin, a marker for both macrophages and neutrophils, and by the absence of the neutrophil-specific marker, myeloperoxidase. To investigate the detailed localization of the bacteria and the NPs in our system, we used two different approaches. First, we took advantage of a transgenic zebrafish line *mpeg1*:mCherry in which macrophages are red fluorescently labeled.[18] In separate experiments, we used the *lyz*:DsRed zebrafish line in which neutrophils are labeled red[19] and, in parallel, we also carried out immunolabeling using L-plastin

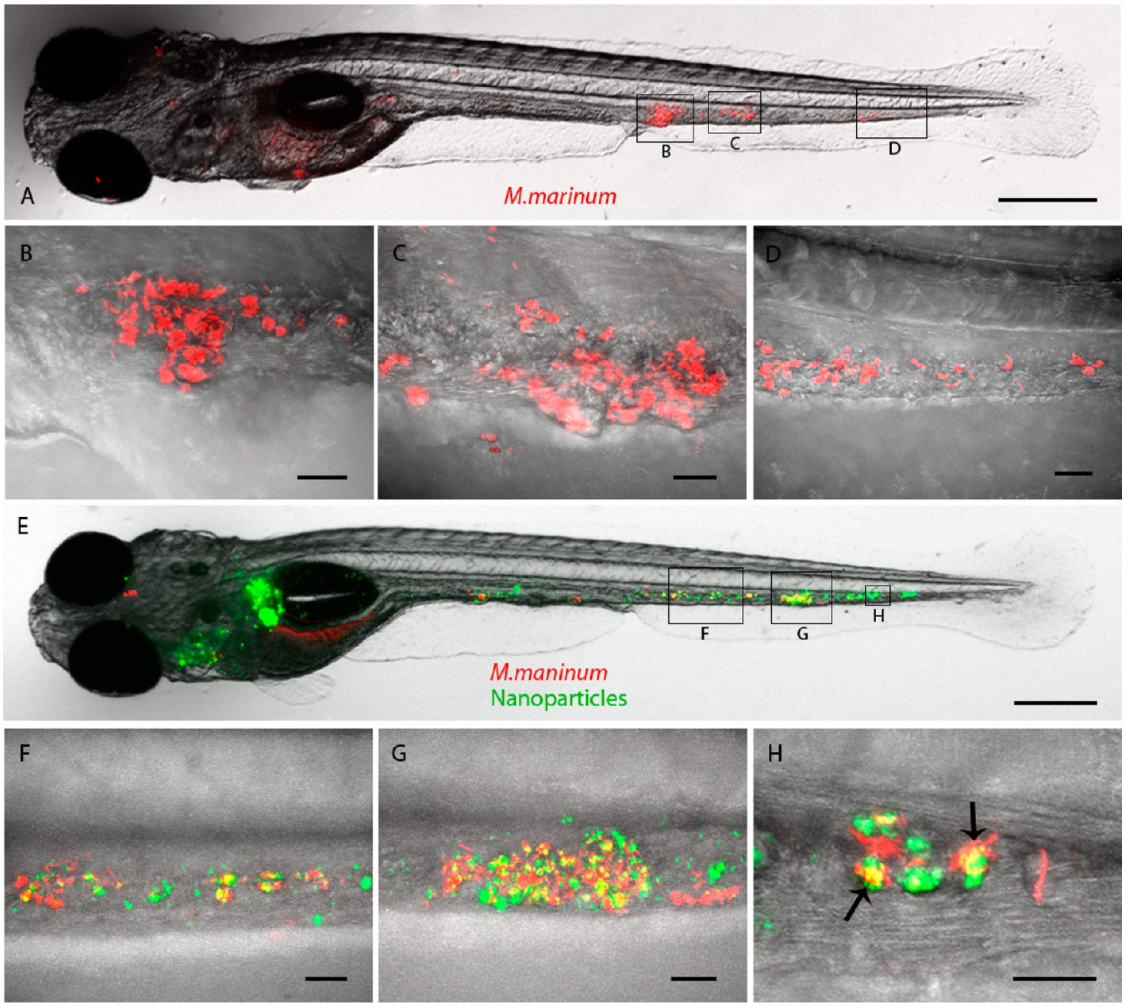

Figure 1. ***M. marinum*** **infection and localization of nanoparticles in their vicinity. (A,E) Lateral views of the whole embryos. (B−D,F−H) Lateral views of selected areas from A and E, respectively; maximal intensity projections. (A)** ***Mycobacterium marinum*** **injected in the posterior caudal vein is able to survive and grow, leading to the formation of granulomas (B,C), as well as individually infected cells (D) 3 dpi. (E) NPs injected in the posterior caudal vein at 3 dpi are able to target granulomas (G) as well as individually infected cells (F). Nanoparticles and mycobacteria are likely to be found in the same cells, as shown by arrows (H). Scale bars: 300 μm (A,E); 20 μm (B−D,F−H).**

antibody.[20] We confirmed that the bacteria were almost exclusively found in macrophages 1−3 dpi (Figure 2A,C and supporting videos 1 and 3); in contrast, only on a few occasions did we find Mm in neutrophils at these time points (result not shown).

When green NPs where injected at 2 dpf into the caudal vein, they efficiently localized within a few hours in *mpeg1*:mCherry-positive cells or *lyz*:DsRed-negative\L-plastin-positive cells, thus indicating macrophages (Figure 2B,D and supporting videos 2 and 4). In subsequent experiments, we analyzed the fate of NPs and Mm injected within the same embryos. When DsRed Mm and fluorescent NPs were injected at 2 and 3 dpf, respectively, they colocalized within L-plastin-positive cells at 4 dpf (Figure 2E and supporting video 5). Next, we injected GFP bacteria (2 dpf) and 1 day later far-red NPs into fish having red macrophages. The green bacteria and the far-red NPs (which appear white in the images) colocalized in red macrophages 1 day later (Figure 2F and supporting video 6). We conclude from these results that both Mm and NPs share the same cellular niche: the macrophage.

We next quantified the percentage of NPs that could be found in cells containing mycobacteria. For this, we first injected zebrafish embryos at 2 dpf with ≈150 cfu of red fluorescent Mm. The day after, we injected coumarin 6 green NPs, and at 7 dpf, we calculated the percentage of NPs found in cells containing bacteria by confocal microscopy (Table 1). This analysis revealed that 82% of the NPs, or clusters of NPs, resided in cells infected with Mm; the remaining NPs localized to noninfected cells. In these experiments, the one-day interval between the injection of bacteria and of the NPs was evidently not sufficient time for the Mm to assemble into granulomas. In a separate experiment, we therefore asked whether NPs could target already developed granulomas, whose assembly requires about 3 days.[13] We therefore waited

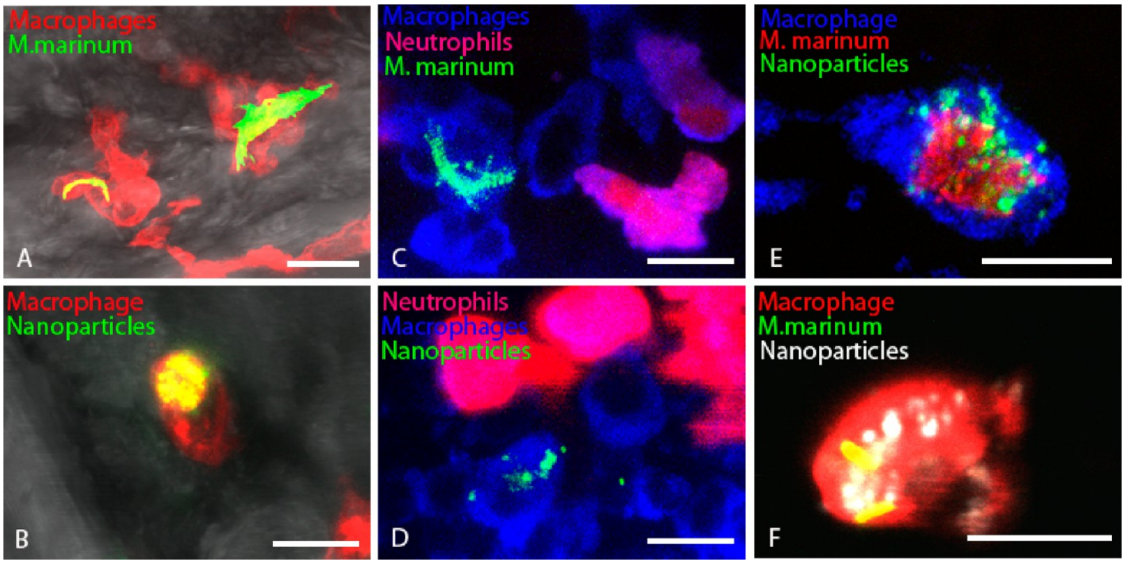

Figure 2. *M. marinum* **and nanoparticles are both found inside macrophages. (A–F) Lateral view of an area of the fish along the posterior caudal cardinal vein; maximal intensity projections. Both green fluorescent Mm and NPs are found within** *mpeg1:cherry* **cells (A,B) as well as in** *lyz*:DsRed-negative/L-plastin-positive cells (C,D). (E) Red Mm and green fluorescent NPs are found colocalize in L-plastin-positive cells. (F) Green Mm and far-red NPs colocalize in *mpeg1:cherry*-positive cells (macrophages). Scale bars: 10 μm. Table 1 shows the percentage of NPs injected at 1 or 3 days postinfection found in clusters within infected macrophages at 5 dpi as assessed by microscopic analysis.

TABLE 1. Quantification of Nanoparticle Clusters in Infected Cells

NPs injected	NP cluster percent in infected cells at day 5 postinfection
1 day postinfection	82%
3 days postinfection	74%

3 days between the injection of Mm and NPs, the latter done at 5 dpf. After an additional 2 days, we analyzed the embryos by confocal microscopy. The results showed that 74% of the injected NPs, or clusters of NPs, were able to access into the preassembled granulomas (Table 1) and into individually infected cells. Thus, phagocytosed NPs are able to reach both assembling and already established granulomas.

Dynamics of M. marinum Infection in the Vasculature and Granuloma. Having seen high levels of colocalization of Mm and NPs within macrophages, we sought to determine the dynamics of this process. It had been concluded by the Ramakrishnan group that once Mm is injected into the circulatory system the bacteria are rapidly phagocytosed and then transported across the blood endothelial barriers deep into tissues; there, they subsequently form granulomas through infection of new uninfected macrophages that are recruited *via* chemotaxis.[13,16] Given the proposed scenario, whereby the granulomas assemble deep in the tissues, we expected that it would take at least several hours for uninfected macrophages containing NPs to migrate through the tissues to reach the granulomas. To our surprise, however, within a few minutes after their injection, the NPs could be directly phagocytosed by *already infected macrophages*. Since we wanted to follow the fate of NPs injected at different times after infection, we realized it was crucial first to understand in detail the timing of bacterial processes following injection. For this, we also took advantage of a fish line expressing the fluorescent marker *fli1*:EGFP, thereby labeling the vasculature green.[21] Blue fluorescent dextran was also used to fill the lumen of the blood vessels (injected 30 min before observation) to follow the fate of red Mm injected at 2 dpf. The embryos were then investigated either as soon as possible (within 15 min) or at various times until 5 dpf (*i.e.*, 3 dpi). We observed that after a few hours the vast majority of bacteria remained confined within the green-lined vasculature (Figure 3A and supporting video 7). Even at this early time point, a few bacteria were invariably found outside the vasculature in macrophages (Figure 3B and supporting video 8). Nevertheless, by 1 dpi, the vast majority of Mm were restricted to the blood system (Figure 3C and supporting video 9); hardly any bacteria were seen outside the vasculature, possibly because these bacteria had been killed. Between 2 and 3 dpi, there were still substantial numbers of Mm within macrophages in the blood vessels (Figure 3D and supporting video 10). Starting from day 3 dpi, an increasing number of bacteria were found outside the vasculature, presumably in macrophages (Figure 3D and supporting video 10). A technical limitation at these time points was the loss of the red fluorescence from the *mpeg1*:mcherry Mm-infected macrophage embryos. By 3 dpi, the first granulomas started to be evident, as previously shown.[13]

Correlative Light and Electron Microscopy of Granulomas. The ultrastructure of the system was investigated to

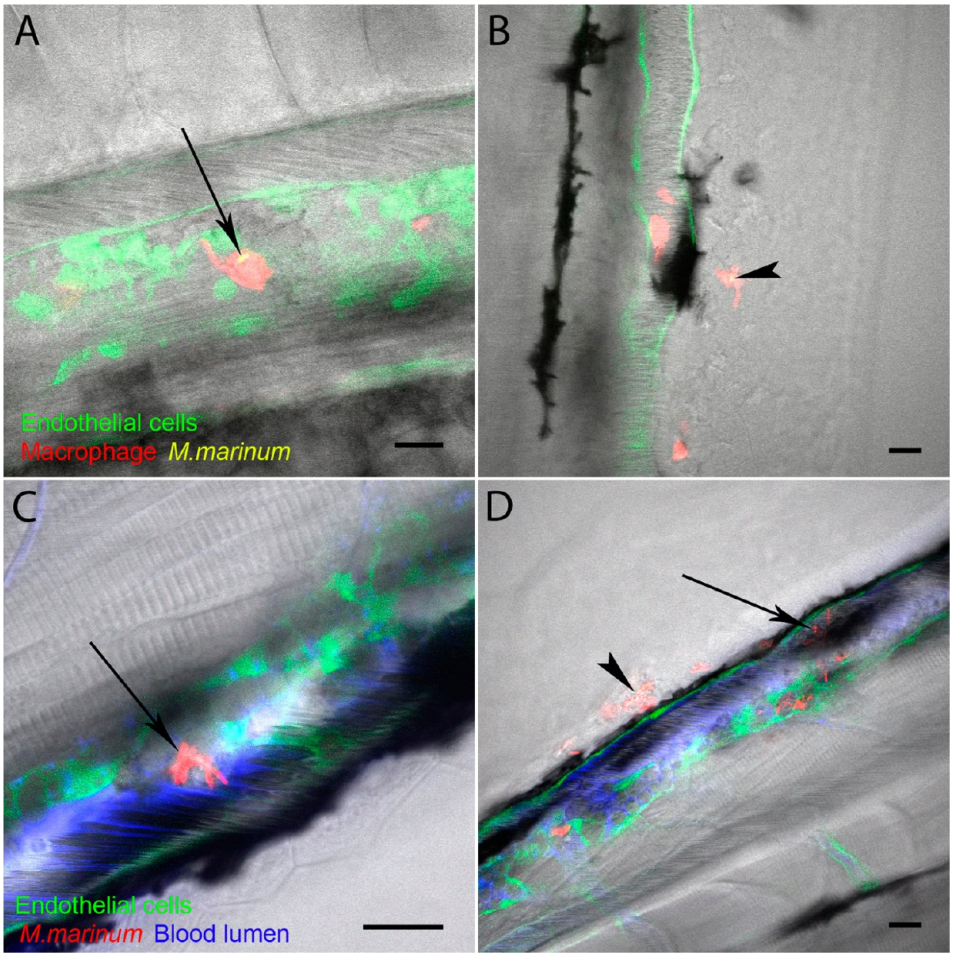

Figure 3. ***M. marinum*** **localization relative the vasculature at different times postinfection. (A−D) Lateral view of an area of the fish along the posterior caudal cardinal vein, single focal plane. (A) Red macrophage infected with green Mm is located within the blood vasculature at 5 hpi. Endothelial cells are labeled green. Image taken from supporting video 7. (B) Mm (green) can occasionally be found outside the vasculature inside red macrophages at 5 hpi. Endothelial cells are labeled green. Image taken from supporting video 8. (C) Red fluorescent Mm localizes within the lumen of the blood vessels at 1 dpi. Endothelial cells surrounding the vessel are labeled green while the lumen is highlighted by blue dextran. Image taken from supporting video 9. (D) Red fluorescent Mm is found both inside and outside the lumen of the vasculature at 3 dpi. Endothelial cells (green), lumen (blue dextran). Arrows indicate intravascular Mm, while arrowheads point at Mm that is found outside the vessels. Image taken from supporting video 10. Scale bars: 15 μm.**

elucidate in more detail how the mycobacteria, the macrophages in granulomas, and the vasculature are organized using electron microscopy. Since the granulomas represent a relatively small fraction of the volume of the embryo, we needed to develop a correlative light-electron microscopy approach. For this, we first infected 2 day old *flil*:EGFP embryos with red Mm for 4 days. These embryos were fixed in paraformaldehyde and prepared for cryostat sectioning. The 20 μm cryo serial sections were prepared and examined by fluorescence microscopy to select sections throughout granulomas. Analysis of these thick sections again confirmed the intimate connectivity between the granuloma and the vasculature (Figure 4A). The selected sections were then embedded in epoxy resin and sectioned for EM. Critically, the solvents used in this approach degrade the PLGA NPs so it was not possible to localize them by EM. Analysis of these sections revealed a number of important features about mycobacteria relative to the granulomas: (1) The granulomas could be found adjacent to, and even within, blood vessels (Figure 4A,B). (2) Occasionally, we could find erythrocytes (which are nucleated in fish) in close apposition with infected macrophages (Figure 4G,H). (3) There were intact macrophages with well-preserved mycobacteria in phagosomes (Figure 4C,D,F). (4) We also saw extensive regions showing large necrotic areas with many extracellular, but well-preserved (presumably alive), mycobacteria (Figure 4E,I). (5) Among the necrotic areas, we observed large lipid-droplet-like structures (Figure 4I). Accumulation of large lipid droplets in human TB granulomas is well-established.[22−24] (6) A significant number of Mm had large lipid bodies in their cytoplasm (Figure 4E,F,I). These structures are also well-established for mycobacteria, including Mtb.[25,26] (7) Finally, we also observed electron-dense granules in the bacterial

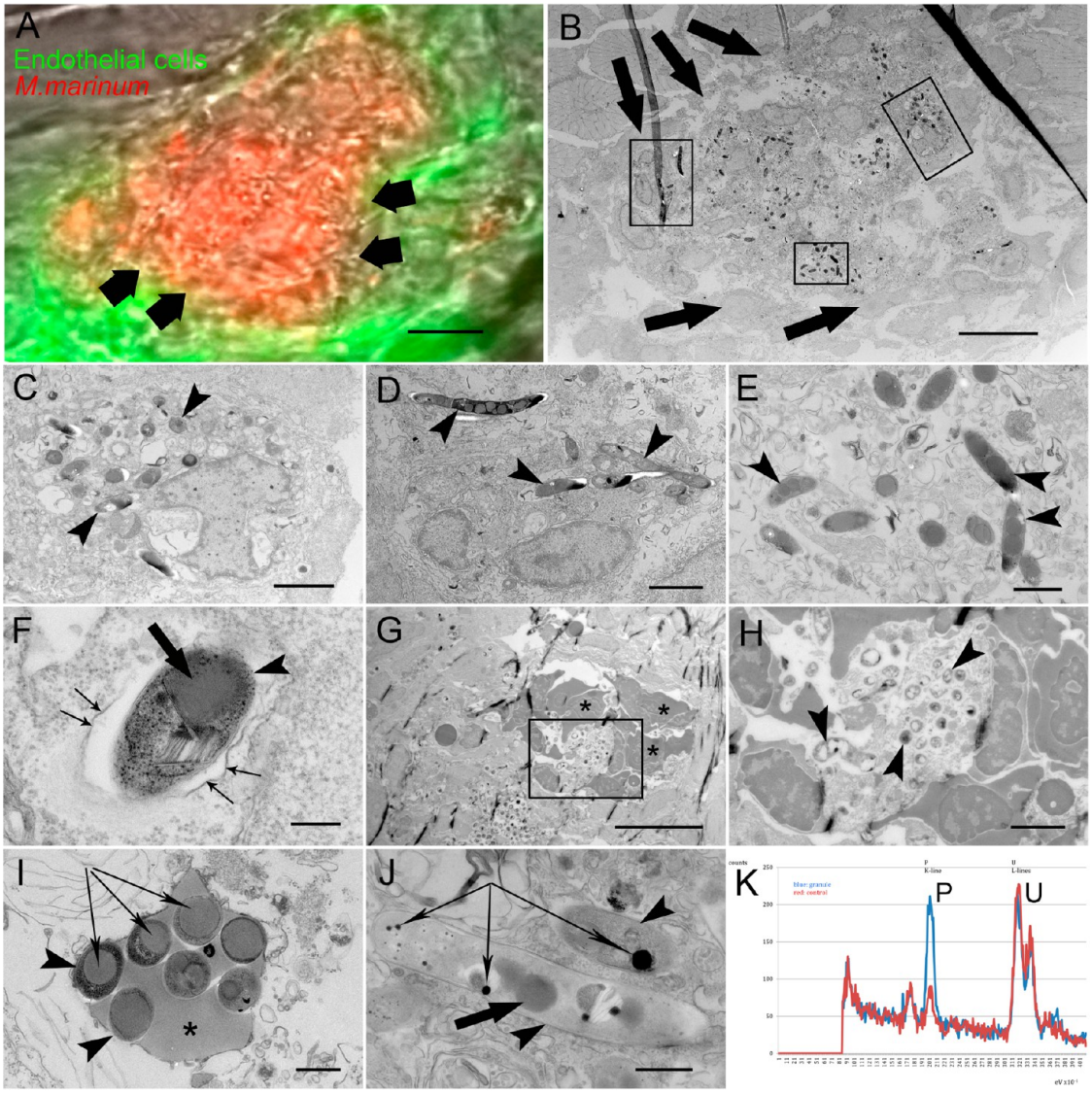

Figure 4. Correlative light microscopy/electron microscopy analysis of granulomas. (A) Granuloma with red Mm is found in direct contact with green fluorescent vasculature in a 20 μm thick cryostat section. (B) Same granuloma is seen in transmission EM in a 70 nm section. Arrows identify endothelium adjacent to the granuloma. (C−E) Enlargements of B. (C,D) Intact macrophages infected with Mm (arrowheads). (E) Bacteria (arrowheads) in a necrotic cell. (F) Mm (arrowhead) with large lipid body (thick arrow) inside a phagosome (thin arrows). (G) Erythrocytes (asterisks) directly adjacent to Mm-rich granuloma in a cryosection. (H) Enlargement of G (Mm identified by arrowheads). (I) Mm (arrowheads) are enmeshed in a large lipid droplet (asterisk) inside a necrotic cell. (J) Mm (arrowheads) having large lipid bodies (thick arrow) and variable sized phosphate granules (thin arrows). (K) X-ray microanalysis spectrum of an area of phosphate granules; the peaks for phosphate (P) and uranium (U, used for freeze substitution) are indicated. Scale bars: 10 μm (A,B,G); 2 μm (C,D,H); 1 μm (E); 500 nm (I,J); 200 nm (F).

cytoplasm (Figure 4J), reminiscent of polyphosphate granules that have been identified in Mtb.[27] The osmium tetroxide necessary for contrast was not compatible with X-ray microanalysis in these preparations. However, using stationary phase-grown Mm that were prepared for cryo-substitution and embedded in Lowicryl resin, we could identify these granules as being enriched in phosphate in sections using X-ray microanalysis (Figure 4K). The significance of this observation requires further study.

Dynamics of Nanoparticle Entry into M. marinum-Infected Macrophages and Granulomas. On the basis of the temporal map of events taken by the mycobacteria, we proceeded to analyze how NPs would behave in this system. For this, we first injected at 2 dpf green Mm into zebrafish having red macrophages, and at 1 dpi, we injected far-red NPs (that appear white in the images). Taking into account our previous finding that Mm localized to the vasculature at 1 dpi, our strategy was to focus on individual infected red-labeled macrophages using high-resolution video microscopy and monitor the fate of the far-red NPs as soon as possible after the NP injection. It was striking to observe a rapid and efficient phagocytic uptake of NPs by green Mm-infected macrophages (Figure 5A−C and supporting video 11). A quantitative analysis of this video revealed

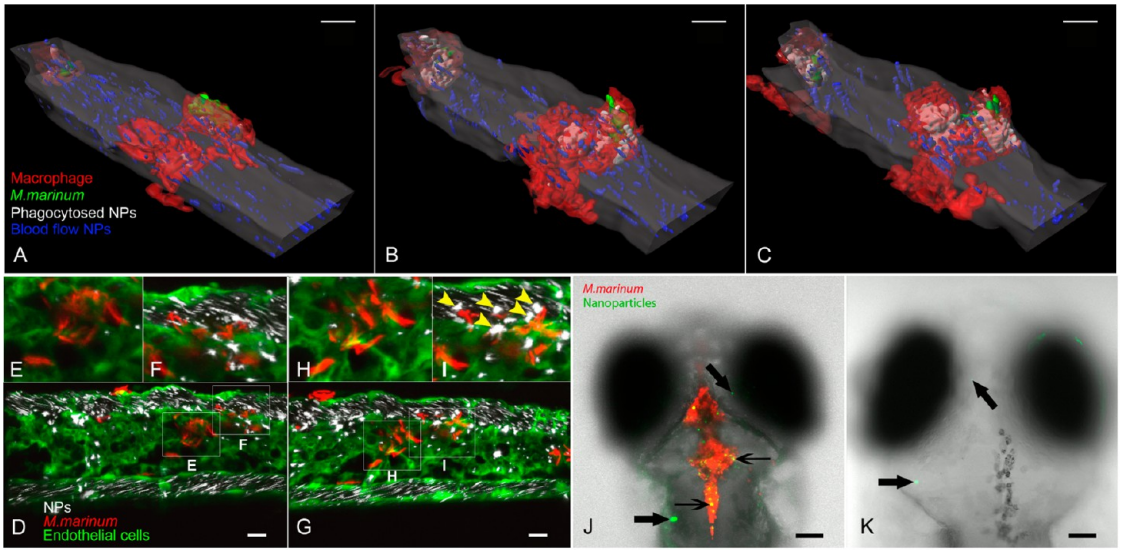

Figure 5. Nanoparticles dynamics in the infected embryo. (A–C) Lateral view of the embryo in the region along the posterior caudal cardinal vein. Far-red NPs when injected 1 day postinfection are rapidly phagocytosed by green Mm-infected red macrophages filling up the cell cytoplasm (images taken from supporting video 11). (D–I) Lateral view of the tail region of the fish, single focal plane. Far-red NPs injected 3 dpi in embryos with green vasculature rapidly reach infected cells that are within the lumen of the vessel (I) but do not reach the red Mm that is not directly in contact with the blood (H). Yellow arrowheads show clusters of NPs that accumulated in time in the vicinity of intravascular mycobacteria (inset, I). Images taken from supporting video 12. (J,K) Dorsal view of the head region of the embryos, maximal intensity projections. Green fluorescent NPs injected 102 hpi in the blood vasculature are able to reach the hindbrain of fish previously injected there with red Mm (J) but not into the hindbrain of control fish previously injected with PVP injection (K). Overlap of green NPs with red bacteria in J appears yellow. Thin and thick arrows indicate NPs in contact and not in contact with Mm, respectively. Scale bars: 8 μm (A–C); 20 μm (D,G); 50 μm (J,K). Table 2 shows the quantification of NP clusters found within the hindbrain at 5 days postinfection. Significance level is indicated as $*p < 0.05$.

TABLE 2. Quantification of Nanoparticles That Reach an Infected or Uninfected Hindbrain Ventricle

fish treatment[a]	mean number of NP clusters found in the hindbrain at day 5 postinfection	standard deviation, standard error of the mean
PVP-injected	0.2778	SD, 0.5745; SEM, 0.1354
Mm-infected	17.78	SD, 27.02; SEM, 6.368

[a] The two treatments are significantly different ($p < 0.05$) with an unpaired t test with Welch correction.

a very high rate of uptake; within ~1 h postinjection, around 24% of the macrophage volume was occupied by NPs (Supporting Information Figure 1) at the last time point. We next analyzed NP localization at 3 dpi, when granulomas are already developed and mycobacteria appear both within and outside the vasculature. At this time point, we had the problem that the mpeg1:mCherry line when infected for 3 days lost their fluorescence. We therefore developed a different strategy. For this, we used the green vasculature fish line, red Mm and injected the far-red NPs. In this experiment, it was evident that within ~1 h NPs colocalize with intravascular bacteria (presumably in macrophages) but were not able to access Mm that had already migrated outside the vasculature (Figure 5D–I and supporting video 12). However, by 24 h after NP injection, a significant fraction of the particles could be found colocalizing with the majority of Mm-infected cells in granulomas, both those accessible to and outside the blood vessels (supporting Figure 2 and supporting video 13).

In order to explain the difference observed at 1 h *versus* 24 h post-NP-injection, we hypothesized that uninfected macrophages would carry NPs to the site of infection by chemotaxis. To investigate this possibility in more detail, we took advantage of the hindbrain ventricle (HV), a chamber separated from the main embryo circulatory system by an endothelial cell layer that resembles a blood brain barrier. This chamber starts to develop around 18 h postfertilization (hpf)[28] and after 30 hpf can be used as a site of injection for Mm that is functionally separated from the main body circulatory system.[13,29] Davis and Ramakrishnan[30] showed that, when Mm is injected into this HV, macrophages from the blood are attracted to the HV after crossing the endothelial barrier. We therefore injected ≈60 red Mm in the HV at 30 hpf, and at 102 hpf, green NPs were injected into the caudal vein. One day later, we found clear evidence of NPs localizing in the hindbrain ventricle (Figure 5J), in contrast to uninfected fish (Figure 5K). This result argues that uninfected macrophages from the blood, after phagocytosing NPs, are attracted to the site of infection. A quantification of the NPs reaching the HV in infected and uninfected embryos showed that a significantly higher amount of NPs

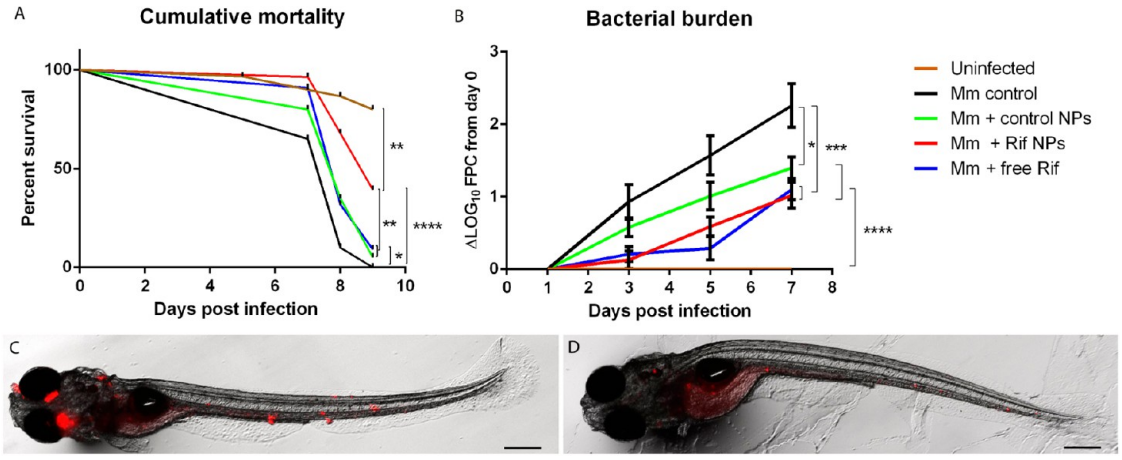

Figure 6. Rifampicin-loaded PLGA nanoparticle efficacy against *M. marinum* infection. (A) Survival of zebrafish embryos injected at 2 dpf with Mm and at 3 dpf with empty PLGA NPs, rifampicin-loaded NPs, free rifampicin or left untreated or uninfected. (B) Fluorescent pixel counts of the bacterial burden of embryos injected at 2 dpf with Mm and at 3 dpf with empty PLGA NPs, rifampicin-loaded NPs, free rifampicin or left untreated or uninfected. (C,D) Lateral view of whole embryos. High variability between fish is evident in the amount of red Mm remaining after the same rifampicin NP treatment at 9 dpi. Scale bars: 300 μm. Significance level is indicated as *$p < 0.05$, **$p < 0.005$, ***$p < 0.001$, ****$p < 0.0001$.

or clusters of NPs reached the HV of the infected embryos, compared to the uninfected ones (Table 2). From these experiments, we can conclude that NPs localize within infected cells, presumably due to both direct phagocytosis by infected and uninfected cells and *via* chemotaxis of uninfected macrophages carrying NPs to the site of infection.

Treatment of the Infection with Rifampicin Enclosing Nanoparticles. Having established that NPs are able to efficiently target infected macrophages, we next asked whether NPs encapsulating rifampicin (mean diameter: 228 nm) could be used to treat the zebrafish embryos infected with Mm. For this, we first monitored the embryo survival. Zebrafish embryos are known to survive for around 10−11 days after Mm infection.[13] Here, embryos were injected with Mm at 2 dpf; 1 day later, we injected 14.4 ng of rifampicin as a free drug or the equivalent amount encapsulated in PLGA NPs. This amount is 12 mg/kg for an embryo weighing 1.2 mg and is therefore equivalent to the amount of drug used in guinea pigs.[31] As controls, we also injected empty (rifampicin-free) NPs or left the fish untreated; an extra group of embryos remained uninfected. As seen in Figure 6, NPs containing rifampicin were able to significantly increase the survival of embryos compared to free drug treated, empty NPs treated, and to the nontreated infected embryos. Nevertheless, the mortality of all these embryos remained significantly higher relative to the uninfected control. Injection of empty NPs or free rifampicin had a slight protective effect, but only the free rifampicin was significantly different from the untreated control. Similar results were obtained when the rifampicin NPs were injected at 3 dpi (supporting Figure 3); however, the therapeutic effect of the NPs was lower than the one obtained with NPs injected at 1 dpi. This is likely due to the emergence of drug-tolerant bacteria.[32] For this reason, we focused the detailed quantitative analysis of the bacterial burden on embryos NP injected at 1 dpi.

We next quantified the bacterial infection. For this, we modified already existing method[32,33] to quantify the Mm infection by measuring bacterial fluorescent pixel counts (fpc) from a large pool of infected embryos (Figure 6B). This approach has been shown to give results that correlate very well quantitatively with cfu data.[32] We used the same treatment groups as for the previous survival experiment (Figure 6A). In this analysis, the uninfected fish had no fluorescent bacterial signal, while the untreated infected larvae showed a 2.26 log increase in fluorescence signal between day 1 (time of NP injection) and 7 dpi or 9 dpf. The injection of free rifampicin lowered the bacterial burden until 5 dpi, but bacterial growth increased dramatically at 7 dpi. In contrast, the rifampicin-loaded NPs gave a consistent reduction in bacterial load over the time of the experiment. After 7 dpi, fish in all treatments started to die, thereby introducing a bias since the more heavily infected embryos died and were no longer included in the analysis. At this time, whereas some fish still had significant bacterial burden, others were effectively cleared of the infection (Figure 6C,D). We argue that the latter shows that the antibiotic NPs are effective in those fish that do not develop significant drug tolerance (phenotypic or nongenetic resistance), whereas the former illustrate the stochastic selection of drug tolerant bacteria in response to rifampicin.[32]

DISCUSSION

The foundation of this study was the striking therapeutic results that have been obtained using biodegradable nanoparticles enclosing antibiotics against

Mtb in different animal models.[8] These data are among the most impressive demonstration of the increased efficacy of NP-based drug delivery compared to conventional drug administration. It seemed likely from the outset that these positive results were related to the fact that macrophages, the cells that most efficiently take up NPs (>200 nm) and MPs,[5] are the same cells where Mtb reside.[8] Nevertheless, until now, none of these studies investigated the fate of the NPs (or MPs) administered by different routes, such as by injection, orally or *via* the lung-aerosol route into Mtb-infected animals. The most obvious reason is that it is not straightforward to image both bacteria and NPs in animals such as mice and guinea pigs, and it is even more complicated to analyze NPs/mycobacteria interactions in real time in these animal models.

In contrast, the zebrafish embryo that we introduce here as a vertebrate model for analyzing NP-mediated drug delivery is a widely used model for an increasing number of biomedical applications, in large part because of its optical transparency. This system allowed us for the first time to visualize in real time the uptake of both fluorescent mycobacteria and NPs in a living vertebrate. Moreover, the availability of transgenic fish with fluorescent macrophages, neutrophils, or blood vessel endothelial cells was an additional strength of this system, which simplified interpretation of the results. The injection of red or green fluorescent Mm into 2 day old embryos led to the rapid and essentially exclusive uptake of bacteria into macrophages that, within 3 days, assembled into granulomas in different parts of the fish body, in agreement with previous findings.[13] Further supporting the claim that Mm infection in zebrafish is a useful model for human TB is the close histological similarity of the adult zebrafish Mm granulomas to those that form with human tuberculosis.[34]

Using this zebrafish model of fish tuberculosis, we administered PLGA NPs that enclosed fluorescent dyes, for localization studies, or rifampicin, for therapy. These NPs were characterized in detail in our recent publication analyzing *M. bovis* BCG in mouse primary macrophages.[12] In that study, the key finding from the point of view of localization was that the fluorescent NPs and the bacteria were found in different compartments within the same cells; the bacteria were in arrested early stage phagosomes (like Mtb), whereas the NPs resided in a phago-lysosomal compartment for many days, in which the fluorescent dye was able to diffuse out into the cytoplasm. This was consistent with the effect of the rifampicin-loaded NPs that, although localized separately from the mycobacteria and administered for only 3 h to the infected macrophages, were able to effectively kill BCG over a period of around 10 days.[12]

One of the major findings of the current study was that when we injected these fluorescent NPs into the fish embryos, we found that within relatively short periods of time they colocalized with the infected cells, both inside the granulomas and in more isolated infected cells. Use of transgenic fish with red fluorescent macrophages revealed that, like for the mycobacteria, these cells were the predominant ones that actively took up the NPs. Earlier studies by the Ramakrishnan group led them to present a model whereby the newly infected macrophages migrate from the blood deep into tissues where they assemble into the granulomas. There they release factors that attract uninfected macrophages *via* chemotaxis to the granulomas.[16] An important role was revealed in these events for proteins expressed by the region of difference (RD-1) locus, a strong virulence determinant in both Mm and Mtb.[35,36] It was also shown that one of the RD-1-encoded proteins, ESAT 6, stimulates the release of a matrix metalloprotease (MMP9) from epithelial cells adjacent to the zebrafish granuloma that facilitates the chemotactic attraction of uninfected macrophages to the infection sites.[37]

Given this previous model on how Mm granulomas assemble deep in tissues in the zebrafish embryo,[16] we were surprised to find that NPs could be taken up by infected macrophages within minutes after they were injected into zebrafish embryos. We therefore investigated the dynamics of both the bacterial infection and the subsequently added NPs in more detail. Use of the transgenic fish with EGFP-labeled endothelial cells, in conjunction with injection of blue fluorescent dextran as a fluid phase blood vessel marker, confirmed that most of the infected macrophages in granulomas had direct access to the blood circulation at 1 dpi, and many still maintained that access at 3 dpi. The intimate interconnections between the granulomas and the circulatory system were seen also in the correlative light and electron microscopy approach we developed to analyze the ultrastructure of the granulomas. The EM analysis also showed the presence of extensive host lipid droplets and bacterial lipid bodies, both reminiscent of those seen in human TB granulomas.[24] The ultrastructural analysis also revealed the presence of both intracellular and extracellular bacteria in necrotic regions. Whereas emphasis is usually given to the fact that Mtb and Mm are intracellular pathogens, these bacteria can be present in high numbers extracellularly in necrotic regions of granulomas.[38] In our infected embryos treated with rifampicin NPs, some fish are almost cleared of the infection 9 dpi whereas others have residual granulomas. The latter are likely to be antibiotic-tolerant bacteria.[32] In those fish where the bacterial are mostly cleared, we assume that the antibiotic released from the NPs reaches both intracellular and extracellular bacteria.

From our results, the overall scenario we propose is that the NPs are taken up by both infected and uninfected macrophages; the latter are attracted to the sites of infection where they can phagocytose infected

macrophages.[13] The NPs are targeted to the phagolysosomes where they release the antibiotic that diffuses into the cytoplasm and then out of the cells,[12] including to the areas of necrosis. This leads to a decrease in bacterial load and enhanced embryo survival. This scenario would also fit with the data of Sharma *et al.*[31] in Mtb-infected guinea pigs, which are known to have extracellular bacteria in necrotic granulomas.[39] In the Sharma *et al.* study,[31] rifampicin NPs administered once either orally or *via* inhalation led to effective clearance of Mtb. This could be correlated with plasma levels of the antibiotic that remained above that needed to kill the bacteria for about 7 days.

Our results suggest that the zebrafish larva/Mm system may be an interesting model for a rare form of tuberculosis in humans referred to as miliary or disseminated TB. This form, which occurs at the rate of 1−3% of human TB cases, is a very severe and lethal form of the disease, whereby the bacteria disseminate *via* the circulation or lymph to essentially any organ, most prominently the lungs, liver, and spleen.[40] In addition, human miliary TB is especially prominent in HIV-infected individuals.[41,42] Patients with miliary TB appear to lack the γ-interferon-mediated (*via* T-helper cells, Th-1) pro-inflammatory response in the lungs and have an elevated level of the anti-inflammatory (Th-2) cytokines IL-4 and IL-10.[43,44] In our model system that lacks adaptive immunity until several weeks after fertilization,[15] the connection between granulomas and blood vasculature is evident from video microscopy and EM data; the vast majority of the granulomas are closely attached to the vasculature (supporting video 7, supporting Figure 2, and Figure 4A). Granulomas that are not directly linked to the vasculature were seldom seen. As in miliary TB, the granulomas in the fish could spread *via* the blood system throughout the body of the zebrafish; in fact, it is possible to see infected cells and free mycobacteria circulate around the blood at all time points, especially in late stages of infection. Since NPs injected in the zebrafish caudal vein efficiently reach infected macrophages, we speculate that intravenous administration of NPs could be beneficial for miliary TB. In agreement with this idea, PLGA NPs of 200 nm size injected in the blood of mice efficiently target the three main organs that are important in miliary TB: spleen, liver, and lungs.[45]

Also in the case of the more typical adult type tuberculosis, we hypothesize that NPs injected in the blood may also be able to target granulomas that are not in direct contact with the blood. This would fit with the data of Dannenberg[46] with BCG in rabbits, which showed evidence of a high turnover of monocytes coming from the blood within a tissue granuloma, even after the onset of adaptive immunity. Moreover, PLGA NPs around 200 nm in size efficiently target the lungs when injected intravenously in the tail of mice,[45] and this scenario could be further improved with careful engineering of NPs' surface and shape.[47] Nevertheless, once the important criteria of high encapsulation and slow release of drugs have been achieved, NPs have a great potential in the treatment of Mtb. Thanks to the efficient targeting to macrophages, NP or MP therapy is also well-suited to encapsulate the so-called "second line" drugs, used for MDR and XDR Mtb, that are generally more toxic.[48] In fact, three of these second line antibiotics, moxifloxacin (NPs)[49] and ofloxacin (NPs)[50] or capreomycin (in MPs),[51] have been successfully encapsulated in different polymers, and the first two were shown to be effective against Mtb in macrophages *in vitro*. It may also be worth considering strategies to target the NP to extracellular mycobacteria, for example, *via* ligands on NPs that bind bacterial surface components; the NPs would then attach to the bacteria and release the antibiotic extracellularly. In this case, the surface of the NPs might need to be conjugated with polyethylene glycol to prevent uptake by macrophages.[6] For such a strategy, the zebrafish model of fish tuberculosis would again be an attractive and accessible system to test this idea.

CONCLUSION

We provide evidence that the zebrafish embryo, in addition to its established strength for visualizing infections such as *Myobacterium marinum*, is also a powerful system for monitoring the interactions of nanoparticles with the infectious organisms and with selected host cells of interest. Imaging of fluorescently labeled NPs provided the foundation for demonstrating that rifampicin-loaded PLGA NPs have therapeutic effects that can be monitored both by quantitation of fluorescent bacteria and of the survival of the embryos.

MATERIALS AND METHODS

Nanoparticle Preparation and Characterization. For detailed explanation of PLGA nanoparticle preparation and characterization, see Kalluru *et al.*[12]

Bacterial Strains Used. *Mycobacterium marinum* was obtained from Lalita Ramakrishnan, carrying fluorescent reporter constructs DsRed or GFP and resistance to kanamycin. Mm was grown in 7H9 medium as previously described in Gao *et al.*[52] Once bacteria reached the exponential phase, they were pelleted, and the bacterial medium was replaced with a solution of polyvinylpyrrolidone (PVP, MW 10 000, Calbiochem) 2% in distilled water in order to obtain the desired bacterial number. The pellet was then thoroughly vortexed for the subsequent injection.

Fish Care and Treatment. The main zebrafish line used was Casper, Tg (nacre −/−; roy −/−). The embryos were kept in Petri dishes at 28.5 °C for each experiment.

The lines Tg(*mpeg1*:mcherry), Tg(*lyz*:DsRed2), and Tg(*fli1*:EGFP) were also used to study NP and Mm localization. For these

zebrafish lines, the embryos were kept in egg water with the addition of phenylthiourea (Aldrich) 0.003%.

These experiments were conducted in agreement with the provisions enforced by the Norwegian national animal research authority (NARA).

Bacterial Injections. In survival and fluorescent pixel count experiments, fish were injected with ≈250 cfu in the posterior (caudal) cardinal vein at 48−52 hpf. In the case of the hindbrain experiment, embryos were injected with ≈60 cfu in the hindbrain ventricle at 32 hpf. In all other experiments, ≈150 cfu was injected into the posterior (caudal) cardinal vein. For each injection, embryos were first anesthetized in tricaine (Finquel, Argent Laboratories) as described in Gao *et al.*[52] and the injection performed after placing the embryo on a gel made of hardened 2% agarose (Sigma) in water.

Injections of Nanoparticles. A solution of PVP 2% in distilled water was added to lyophilized NPs in order to obtain the required concentration for injections. The NPs were then bath-sonicated for 5 min before being administrated to the zebrafish larvae. In survival and FPC experiments, we injected 3 nL of 14.4 mg/mL suspension of NPs. In all the other experiments, we injected 1 nL. All the injections of NPs were performed in the posterior (caudal) cardinal vein at 72 or 120 hpf with the sole exception of the hindbrain experiment when NPs were injected at 102 hpf.

L-Plastin Antibody Staining. For detailed explanation, see Cui *et al.*[20]

Injections and Microscopy. Embryos were injected using a glass needle (Harvard apparatus) controlled with a micromanipulator Narishige MN-153 connected to an Eppendorf FemtoJet express. Microscopic visualization of the fish during injections was facilitated by a stereomicroscope Leica DFC365FX with a 1.0X Planapo lens that was also used for fluorescence pixel count analysis and for imaging of the whole embryo (Figure 1A,E and Figure 6C,D). An Olympus FluoView 1000 upright BX61WI confocal microscope was used for high-resolution microscopic imaging. For imaging with this microscope, embryos were sedated embryos and first anesthetized in tricaine (Finquel, Argent Laboratories) as described in Gao *et al.*[52] Subsequently, they were placed in a small dish with a glass bottom that was filled with low melting point agarose. Once the agarose had hardened, egg water was added to the dish and water lens used for visualization. We used a 10× lens for the image in Figure 5J,K and a 60× lens for all other images and videos. In Mm localization experiments, the blue dye Dextran (MW 10 000) was used. Imaris software was used for Figure 5A−C and supporting videos 1−6, 9, and 11−13. Supporting videos are all shown at 7 fps. The acquisition time for the supporting videos 7, 8, 11, and 12 were 14, 10, 49, and 48 min, respectively. The laser lines for fluorescence imaging used were 405 (blue), 488 (green), 543 (red), and 647 (far red).

Correlative LM and EM. Larvae were fixed with 4% paraformaldehyde in 60 mM HEPES buffer for 24 h at 4 °C, infiltrated with 2.3 M sucrose in PBS for 24 h at 4 °C, then placed in plastic trays, covered with Tissue-Tek OCT compound, and immediately frozen in liquid N_2. Twenty micrometer sections were made using a Leica CM1950 cryostat and placed on a polylysine-coated glass bottom dish No. 2 (MatTek Corp.) with a laser-printed finder grid. Sections were inspected using a Leica DM IRBE inverted fluorescence microscope and imaged using a DFC 350 FX side-mounted camera. Selected thick sections were further fixed overnight with 4% PFA and 0.5% glutaraldehyde in 60 mM HEPES buffer before processing for Epon embedding in glass dishes. After polymerization, the block had an imprint of the finder grid so that tissue of interest could be located. Sectioning was done with a Leica UCT ultramicrotome with the feed set to 70 nm. Sections were inspected using a Philips CM100 electron microscope and imaged using an Olympus Quemesa 11 megapixel CCD TEM camera. Some embryos were processed for Tokuyasu cryosections.[12]

X-ray Microanalysis. High-pressure frozen, freeze-substituted stationary phase cultures of Mm were embedded in Epon, and sections of 200 nm were examined in a Philips CM12 transmission electron microscope equipped with a Megaview digital camera. X-ray microanalysis was performed using an EDAX (Phoenix) X-ray detector and TEM Quant Materials software.

Survival Study. Zebrafish embryos were injected at 48−52 hpf with ≈250 cfu of DS red Mm. At 72−76 hpf, embryos were injected with either free rifampicin (14.4 ng administered, diluted in a solution of 5% DMSO in 2% PVP) or NPs containing rifampicin (14.4 ng administered, NPs diluted in a solution 2% PVP, DMSO was omitted as this would dissolve the NP) or empty NPs or were left untreated. A fish was considered dead when its heart stopped beating.

Fluorescent Pixel Count. In this experiment, zebrafish embryos were injected at 2 dpf with Mm and at 3 dpf with fluorescent NPs. At 3 dpf and prior to NP injection, each fish was imaged to establish the zero time point. Then, images were taken at 1, 3, 5, and 7 dpi. The imaging of the whole embryo focused on the caudal vein, always with the same settings. In order to distinguish every fish, embryos were kept separated throughout the whole experiment. Subsequently, the 16 bit images were processed with ImageJ, and a "rolling ball" background subtraction "20 pxl" was applied. Next, an objects counter analysis was performed to identify fluorescent elements. The threshold value was set between the lowest gray value of true signal (fluorescent Mm signal) and highest value of background signal (noninfected larvae). The analysis of each object in a picture gives the fluorescent pixel count of each individual zebrafish reflecting the bacterial burden.

Statistics Used. The statistical analysis was carried out using the software GraphPad Prism 6. In HV experiments, we did an unpaired *t* test with Welch correction. In survival experiments, we performed a Log-rank (Mantel-Cox) test. For the fpc analysis, a one-way ANOVA was performed on the delta log fpc data at 6 dpi. There was a significant difference between groups, so we ran a posthoc Tukey multiple-comparisons analysis. Significance level is indicated as $*p < 0.05$, $**p < 0.005$, $***p < 0.001$, $****p < 0.0001$.

Conflict of Interest: The authors declare no competing financial interest.

Acknowledgment. We thank Jan Roger Torp, Ana Tavara, and Peter Alestrøm for their support with zebrafish maintenance. We received excellent support from the IBV light microscopy and EM imaging platforms. We thank Gopal Khuller and his group for their support. We thank Jean-Pierre Levraud and Graham Lieschke for the mpeg1:cherry fish, James Lorens for the fli1:EGFP fish, Phil Croisier for the lyz:DsRed fish lines, and Paul Martin for the L-plastin antibody. During the establishment of the infection model, we received generous support from Lalita Ramakrishnan and her group, especially David Tobin and Kevin Takaki. We thank Maximiliano Gutierrez and Urska Repnik for constructive comments. The project was financially supported by a Norwegian research council Frimedbio grant and a University of Oslo MLS PhD fellowship to F.F. D.W. would like to thank Beatrice Lowe and the MRC for funding. A.H.M. and M.W. were supported by the Smart Mix Program of The Netherlands Ministry of Economic Affairs and The Ministry of Education, Culture and Science.

Supporting Information Available: Additional figures and videos as described in text. This material is available free of charge *via* the Internet at http://pubs.acs.org.

REFERENCES AND NOTES

1. Russell, D. G. Who Puts the Tubercle in Tuberculosis? *Nat. Rev. Microbiol.* **2007**, *5*, 39–47.
2. Flynn, J. L.; Chan, J.; Lin, P. L. Macrophages and Control of Granulomatous Inflammation in Tuberculosis. *Mucosal Immunol.* **2011**, *4*, 271–278.
3. Young, D. B.; Perkins, M. D.; Duncan, K.; Barry, C. E., III. Confronting the Scientific Obstacles to Global Control of Tuberculosis. *J. Clin. Invest.* **2008**, *118*, 1255–1265.
4. Zumla, A.; Nahid, P.; Cole, S. T. Advances in the Development of New Tuberculosis Drugs and Treatment Regimens. *Nat. Rev. Drug Discovery* **2013**, *12*, 388–404.
5. Desjardins, M.; Griffiths, G. Phagocytosis: Latex Leads the Way. *Curr. Opin. Cell. Biol.* **2003**, *15*, 498–503.

6. Wattendorf, U.; Merkle, H. P. PEGylation as a Tool for the Biomedical Engineering of Surface Modified Microparticles. *J. Pharm. Sci.* **2008**, *97*, 4655–4669.
7. Russell, D. G. *Mycobacterium tuberculosis* and the Intimate Discourse of a Chronic Infection. *Immunol. Rev.* **2011**, *240*, 252–268.
8. Griffiths, G.; Nystrom, B.; Sable, S. B.; Khuller, G. K. Nanobead-Based Interventions for the Treatment and Prevention of Tuberculosis. *Nat. Rev. Microbiol.* **2010**, *8*, 827–834.
9. Ranjita, S.; Loaye, A.; Khalil, M. Present Status of Nanoparticle Research for Treatment of Tuberculosis. *J. Pharm. Pharm. Sci.* **2011**, *14*, 100–116.
10. Sosnik, A.; Carcaboso, A. M.; Glisoni, R. J.; Moretton, M. A.; Chiappetta, D. A. New Old Challenges in Tuberculosis: Potentially Effective Nanotechnologies in Drug Delivery. *Adv. Drug Delivery Rev.* **2010**, *62*, 547–559.
11. Pandey, R.; Khuller, G. K. Polymer Based Drug Delivery Systems for Mycobacterial Infections. *Curr. Drug Delivery* **2004**, *1*, 195–201.
12. Kalluru, R.; Fenaroli, F.; Westmoreland, D.; Ulanova, L.; Maleki, A.; Roos, N.; Paulsen Madsen, M.; Koster, G.; Egge-Jacobsen, W.; Wilson, S.; *et al.* Poly(lactide-*co*-glycolide)-Rifampicin Nanoparticles Efficiently Clear Mycobacterium Bovis Bcg Infection in Macrophages and Remain Membrane-Bound in Phago-lysosomes. *J. Cell Sci.* **2013**, *126*, 3043–3054.
13. Davis, J. M.; Clay, H.; Lewis, J. L.; Ghori, N.; Herbomel, P.; Ramakrishnan, L. Real-Time Visualization of Mycobacterium–Macrophage Interactions Leading to Initiation of Granuloma Formation in Zebrafish Embryos. *Immunity* **2002**, *17*, 693–702.
14. Ramakrishnan, L. Looking within the Zebrafish To Understand the Tuberculous Granuloma. *Adv. Exp. Med. Biol.* **2013**, *783*, 251–266.
15. Meijer, A. H.; Spaink, H. P. Host–Pathogen Interactions Made Transparent with the Zebrafish Model. *Curr. Drug Targets* **2011**, *12*, 1000–1017.
16. Lesley, R.; Ramakrishnan, L. Insights into Early Mycobacterial Pathogenesis from the Zebrafish. *Curr. Opin. Microbiol.* **2008**, *11*, 277–283.
17. Clay, H.; Davis, J. M.; Beery, D.; Huttenlocher, A.; Lyons, S. E.; Ramakrishnan, L. Dichotomous Role of the Macrophage in Early Mycobacterium Marinum Infection of the Zebrafish. *Cell Host Microbe* **2007**, *2*, 29–39.
18. Ellett, F.; Pase, L.; Hayman, J. W.; Andrianopoulos, A.; Lieschke, G. J. Mpeg1 Promoter Transgenes Direct Macrophage-Lineage Expression in Zebrafish. *Blood* **2011**, *117*, e49–e56.
19. Hall, C.; Flores, M. V.; Storm, T.; Crosier, K.; Crosier, P. The Zebrafish Lysozyme C Promoter Drives Myeloid-Specific Expression in Transgenic Fish. *BMC Dev. Biol.* **2007**, *7*, 42.
20. Cui, C.; Benard, E. L.; Kanwal, Z.; Stockhammer, O. W.; van der Vaart, M.; Zakrzewska, A.; Spaink, H. P.; Meijer, A. H. Infectious Disease Modeling and Innate Immune Function in Zebrafish Embryos. In *The Zebrafish: Disease Models and Chemical Screens*, 3rd ed.; Detrich, H. W., Westerfield, M., Zon, L. I., Eds.; Elsevier: Oxford, UK, 2011; Vol. 105, pp 273–308.
21. Lawson, N. D.; Weinstein, B. M. *In Vivo* Imaging of Embryonic Vascular Development Using Transgenic Zebrafish. *Dev. Biol.* **2002**, *248*, 307–318.
22. Hunter, R. L.; Jagannath, C.; Actor, J. K. Pathology of Postprimary Tuberculosis in Humans and Mice: Contradiction of Long-Held Beliefs. *Tuberculosis* **2007**, *87*, 267–278.
23. Peyron, P.; Vaubourgeix, J.; Poquet, Y.; Levillain, F.; Botanch, C.; Bardou, F.; Daffe, M.; Emile, J. F.; Marchou, B.; Cardona, P. J.; *et al.* Foamy Macrophages from Tuberculous Patients' Granulomas Constitute a Nutrient-Rich Reservoir for *M. tuberculosis* Persistence. *PLoS Pathog* **2008**, *4*, e1000204.
24. Russell, D. G.; Cardona, P. J.; Kim, M. J.; Allain, S.; Altare, F. Foamy Macrophages and the Progression of the Human Tuberculosis Granuloma. *Nat. Immunol.* **2009**, *10*, 943–948.
25. Daniel, J.; Maamar, H.; Deb, C.; Sirakova, T. D.; Kolattukudy, P. E. *Mycobacterium tuberculosis* Uses Host Triacylglycerol to Accumulate Lipid Droplets and Acquires a Dormancy-like Phenotype in Lipid-Loaded Macrophages. *PLoS Pathog.* **2011**, *7*, e1002093.
26. Stehr, M.; Elamin, A. A.; Singh, M. Cytosolic Lipid Inclusions Formed during Infection by Viral and Bacterial Pathogens. *Microbes Infect.* **2012**, *14*, 1227–1237.
27. Ward, S. K.; Heintz, J. A.; Albrecht, R. M.; Talaat, A. M. Single-Cell Elemental Analysis of Bacteria: Quantitative Analysis of Polyphosphates in Mycobacterium Tuberculosis. *Front. Cell. Infect. Microbiol.* **2012**, *2*, 63.
28. Lowery, L. A.; Sive, H. Initial Formation of Zebrafish Brain Ventricles Occurs Independently of Circulation and Requires the Nagie Oko and Snakehead/Atp1a1a.1 Gene Products. *Development* **2005**, *132*, 2057–2067.
29. Benard, E. L.; van der Sar, A. M.; Ellett, F.; Lieschke, G. J.; Spaink, H. P.; Meijer, A. H. Infection of Zebrafish Embryos with Intracellular Bacterial Pathogens. *J. Vis. Exp.* **2012**, e3781.
30. Davis, J. M.; Ramakrishnan, L. The Role of the Granuloma in Expansion and Dissemination of Early Tuberculous Infection. *Cell* **2009**, *136*, 37–49.
31. Sharma, A.; Sharma, S.; Khuller, G. K. Lectin-Functionalized Poly(lactide-*co*-glycolide) Nanoparticles as Oral/Aerosolized Antitubercular Drug Carriers for Treatment of Tuberculosis. *J. Antimicrob. Chemother.* **2004**, *54*, 761–766.
32. Adams, K. N.; Takaki, K.; Connolly, L. E.; Wiedenhoft, H.; Winglee, K.; Humbert, O.; Edelstein, P. H.; Cosma, C. L.; Ramakrishnan, L. Drug Tolerance in Replicating Mycobacteria Mediated by a Macrophage-Induced Efflux Mechanism. *Cell* **2011**, *145*, 39–53.
33. Stoop, E. J.; Schipper, T.; Huber, S. K.; Nezhinsky, A. E.; Verbeek, F. J.; Gurcha, S. S.; Besra, G. S.; Vandenbroucke-Grauls, C. M.; Bitter, W.; van der Sar, A. M. Zebrafish Embryo Screen for Mycobacterial Genes Involved in the Initiation of Granuloma Formation Reveals a Newly Identified Esx-1 Component. *Dis. Models & Mech.* **2011**, *4*, 526–536.
34. Swaim, L. E.; Connolly, L. E.; Volkman, H. E.; Humbert, O.; Born, D. E.; Ramakrishnan, L. Mycobacterium Marinum Infection of Adult Zebrafish Causes Caseating Granulomatous Tuberculosis and Is Moderated by Adaptive Immunity. *Infect. Immun.* **2006**, *74*, 6108–6117.
35. Ramakrishnan, L. Revisiting the Role of the Granuloma in Tuberculosis. *Nat. Rev. Immunol.* **2012**, *12*, 352–366.
36. Volkman, H. E.; Clay, H.; Beery, D.; Chang, J. C. W.; Sherman, D. R.; Ramakrishnan, L. Tuberculous Granuloma Formation Is Enhanced by a Mycobacterium Virulence Determinant. *PLoS Biol.* **2004**, *2*, 1946–1956.
37. Volkman, H. E.; Pozos, T. C.; Zheng, J.; Davis, J. M.; Rawls, J. F.; Ramakrishnan, L. Tuberculous Granuloma Induction *via* Interaction of a Bacterial Secreted Protein with Host Epithelium. *Science* **2010**, *327*, 466–469.
38. Hunter, R. L. Pathology of Post Primary Tuberculosis of the Lung: An Illustrated Critical Review. *Tuberculosis* **2011**, *91*, 497–509.
39. Hoff, D. R.; Ryan, G. J.; Driver, E. R.; Ssemakulu, C. C.; De Groote, M. A.; Basaraba, R. J.; Lenaerts, A. J. Location of Intra- and Extracellular *M. tuberculosis* Populations in Lungs of Mice and Guinea Pigs during Disease Progression and after Drug Treatment. *PLoS One* **2011**, *6*, e17550.
40. Sharma, S. K.; Mohan, A.; Sharma, A. Challenges in the Diagnosis & Treatment of Miliary Tuberculosis. *Indian J. Med. Res.* **2012**, *135*, 703–730.
41. Myers, J. N. Miliary, Central Nervous System, and Genitourinary Tuberculosis. *DM, Dis.–Mon.* **2007**, *53*, 22–31.
42. Ray, S.; Talukdar, A.; Kundu, S.; Khanra, D.; Sonthalia, N. Diagnosis and Management of Miliary Tuberculosis: Current State and Future Perspectives. *Ther. Clin. Risk Manage.* **2013**, *9*, 9–26.
43. Sharma, P. K.; Saha, P. K.; Singh, A.; Sharma, S. K.; Ghosh, B.; Mitra, D. K. Foxp3+ Regulatory T Cells Suppress Effector T-Cell Function at Pathologic Site in Miliary Tuberculosis. *Am. J. Respir. Crit. Care Med.* **2009**, *179*, 1061–1070.
44. Sharma, S. K.; Mitra, D. K.; Balamurugan, A.; Pandey, R. M.; Mehra, N. K. Cytokine Polarization in Miliary and Pleural Tuberculosis. *J. Clin. Immunol.* **2002**, *22*, 345–352.

45. Mohammad, A. K.; Reineke, J. J. Quantitative Detection of PLGA Nanoparticle Degradation in Tissues Following Intravenous Administration. *Mol. Pharm.* **2013**, *10*, 2183–2189.
46. Dannenberg, A. M. Macrophage Turnover, Division and Activation within Developing, Peak and "Healed" Tuberculous Lesions Produced in Rabbits by Bcg. *Tuberculosis* **2003**, *83*, 251–260.
47. Kolhar, P.; Anselmo, A. C.; Gupta, V.; Pant, K.; Prabhakarpandian, B.; Ruoslahti, E.; Mitragotri, S. Using Shape Effects To Target Antibody-Coated Nanoparticles to Lung and Brain Endothelium. *Proc. Natl. Acad. Sci. U.S.A.* **2013**, *110*, 10753–10758.
48. Smith, J. P. Nanoparticle Delivery of Anti-Tuberculosis Chemotherapy as a Potential Mediator against Drug-Resistant Tuberculosis. *Yale J. Biol. Med.* **2011**, *84*, 361–369.
49. Kisich, K. O.; Gelperina, S.; Higgins, M. P.; Wilson, S.; Shipulo, E.; Oganesyan, E.; Heifets, L. Encapsulation of Moxifloxacin within Poly(butyl cyanoacrylate) Nanoparticles Enhances Efficacy against Intracellular *Mycobacterium tuberculosis*. *Int. J. Pharm.* **2007**, *345*, 154–162.
50. Hwang, S. M.; Kim, D. D.; Chung, S. J.; Shim, C. K. Delivery of Ofloxacin to the Lung and Alveolar Macrophages *via* Hyaluronan Microspheres for the Treatment of Tuberculosis. *J. Controlled Release* **2008**, *129*, 100–106.
51. Giovagnoli, S.; Blasi, P.; Schoubben, A.; Rossi, C.; Ricci, M. Preparation of Large Porous Biodegradable Microspheres by Using a Simple Double-Emulsion Method for Capreomycin Sulfate Pulmonary Delivery. *Int. J. Pharm.* **2007**, *333*, 103–111.
52. Gao, L. Y.; Manoranjan, J. Laboratory Maintenance of Mycobacterium Marinum. *Current Protocols in Microbiology*; Wiley: New York, 2005; Chapter 10, Unit 10B.11.